A computational study of photoisomerization in $Al_3O_3^-$ clusters

X.-Y. Cui and I. Morrison[a)]
Institute for Materials Research, University of Salford, M5, 4WT, United Kingdom

J.-G. Han
National Synchrotron Radiation Laboratory, University of Science and Technology of China, Hefei, Anhui, 230026, People's Republic of China

(Received 1 March 2002; accepted 19 April 2002)

Ab initio calculations are employed to understand the photoisomerization process in small $Al_3O_3^-$ clusters. This process is the first example of a photoinduced isomerization observed in an anion cluster gas-phase system. Potential energy surfaces for the ground state and the excited state (S_1 and T_1) are explored by means of B3LYP, MP2, CI-singles, and CASSCF methods. We demonstrate that the isomerization process occurs between the global minimum singlet state Book structure (C_{2v}, $^1A_1$) and the triplet state Ring structure (C_{2v}, $^3B_2$). The calculated vertical excitation energy is 3.62 eV at the CASSCF level of approximation, in good agreement with the experimental value (3.49 eV). A nonplanar conical intersection, which hosts the intersystem crossing between the S_1 and T_1 surfaces is identified at the region of around $R(1,6)=2.4$ Å. Beyond the experimental results, we predict, that this isomerization is reversible upon absorption of a phonon with energy of 1.92 eV. Our results describe a unique system, whose structure depends on its spin multiplicity; it exists as the Book structure on singlet states and as the Ring structure on triplet states. © *2002 American Institute of Physics.* [DOI: 10.1063/1.1484387]

I. INTRODUCTION

Photoisomerization is an important field in photochemistry involving chemical change brought about by the action of visible or ultraviolet radiation. These processes generally involve the direct participation of electronically excited states of a molecule.[1,2] Some of these processes are vital to the understanding of some topics in the life sciences and some are used for novel single molecule electronic devices.[3–6] In the past decade, great efforts have been made to study the mechanism of photoisomerization both experimentally and theoretically.[7–9] From a theoretical point of view, the central issue to understanding the photoisomerization mechanism lies in the exploration of the potential energy surfaces (PES) for both ground states and excited states. This is due to the fact that the general feature of this type of reaction is the presence of the low-lying intersections (crossings) between the relevant excited state and ground state surfaces that play a fundamental role in the process. Such crossings, conical intersections in the case of two singlet (or two triplet) surfaces, or singlet–triplet surface intersections, provide a very efficient funnel for controlling the evolution of a photoexcited molecule from the Franck–Condon region to the photoproduct valleys.[10,11]

Compared with ample cases found and studied in organic species, for example, the well-known *cis–trans* isomerization, few such cases have been reported in inorganic systems. Chaquin *et al.*[12] performed experimental and theoretical studies of the XYO (X, Y=Cl, Br) light-induced interconversion in an argon matrix. They reported that visible irradiation between 633–700 nm transforms ClBrO into BrClO and above 700 nm the transformation continues into BrOCl. Optimal control of the photoisomerization of Li_2Na via an electronically excited state from the stable acute to the obtuse triangular configuration was simulated by Manz *et al.*[13] Very recently, Hartmann *et al.*[14] reported that a small Na_3F_2 cluster could change into its isomer by the breaking of one metallic and one ionic bond upon absorption of light. This reaction represents the first example of a five-atom cluster gas phase system exhibiting a conical intersection between the ground state and the first excited state.[15]

Photoisomerization in the $Al_3O_3^-$ represents the first example that such photoinduced reactions happen in anion cluster gas-phase systems, and was first observed in photoelectron spectroscopy in 1998 by Wu *et al.*[16] Soon after, Ghanty and Davidson[17] made a theoretical study on this system to interpret the photoelectron spectra and reported some equilibrium geometries of the ground states. However, no attempt has been made to understand the photoisomerization process. For this photoinduced reaction there are two fundamental questions that still remain unsolved. First, which two isomers are responsible for this reaction, i.e., which isomers are the reactant and product? Second, how does this process happen, i.e., what is reaction mechanism? These questions represent a challenge for both theorists and experimentalists. Computational chemistry has already secured its position as an indispensable tool for rationalizing and understanding many features of photoisomerization reactions. In this paper we employ quantum chemistry techniques to provide an understanding of this photoisomerization process and compare our theoretical results with the experimental data. To the best

a)Author to whom correspondence should be addressed. Electronic mail: i.morrison@salford.ac.uk

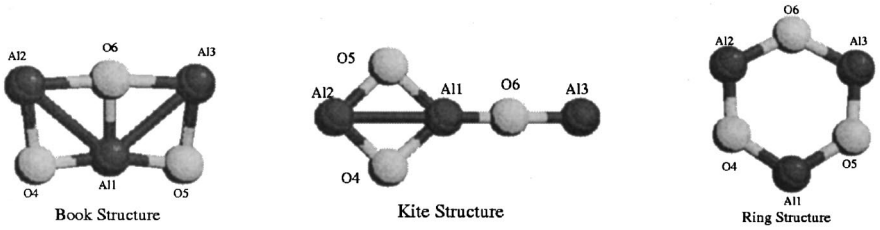

FIG. 1. Structures of the three most stable $Al_3O_3^-$ isomers (see Table I for parameters).

of our knowledge, this present work is the first attempt to understand this novel process.

The paper is structured as follows: In Sec. II, we outline the details of computational methods used in this study. The main results are presented in Sec. III. First, full optimization calculations are performed to obtain the geometrical and electronic structure of all possible candidate isomers in this reaction. Calculated electronic affinities (EA) and vibrational frequencies are compared with the experimental data and potential energy surfaces for the ground singlet and triplet states are mapped. The agreement between our calculated results and experimental data indicates the relevant isomers in the reaction. Population analysis is also employed to understand the charge distribution and charge transfer. Second, an excited states (S_1 and T_1) study is performed to obtain the excited state topology and a conical intersection point is identified. The calculated vertical excitation energy is in good agreement with the experimental value. Based on the exploration of the potential energy surfaces, we then provide a simple model to interpret the photoisomerization reaction mechanism in $Al_3O_3^-$ clusters. Beyond the experimental results, we predict that such isomerization process is, in principle, reversible upon absorption a phonon with energy of 1.9 eV. A discussion is presented in Sec. IV, and Sec. V contains brief conclusive remarks.

II. COMPUTATIONAL DETAILS

Small aluminum oxide clusters present a challenge to theory, as both covalent and ionic bonding is present.[18] Ground state calculations were performed at two levels of approximation: one is the Møller–Plesset second order MP2 method,[19] the other is the hybrid density functional theory incorporating Becke's three parameter exchange functional with gradient correlations provided by the LYP correlation functional (the B3LYP method[20,21]). We demonstrate, as will be shown later, that the semilocal B3LYP approximation offers a better description of these species, so the general conclusions are drawn from B3LYP results. For the excited states calculations, two methods were employed in this study: one is the single-excitation configuration interactions (CI-singles),[22] and the other one is the complete active space multiconfiguration self-consistent field (CASSCF).[23] The CI-singles method was used for numerical calculations along the reaction pathway and to obtain the potential energy surfaces, while the CASSCF method was used to refine the key points and calculate the vertical excitation energy. More importantly, CASSCF ground and excited states calculations serve as the bridges, which link the ground energy surface and the excited energy surface. In CASSCF calculations, the active spaces were constructed with four π orbitals/four active electrons for singlet states, and with six π orbitals/six active electrons for triplet states.

Geometry optimization is a particularly important issue in this work. Full optimization is performed to locate the stationary point on the potential surface using Cartesian coordinates. Partial optimization is performed to obtain the information along the reaction pathway using internal coordinates. Harmonic vibrational frequency analysis was performed for both ground states and excited states to determine the nature of the stationary points. If an imaginary frequency mode appeared, further relaxation was carried to locate to the minimum.

The prediction of properties is usually sensitive to the choice of basis set, particularly for the excited states, hence all the final results reported in this study were provided by employing the large standard basis set 6-31++G(p,d). All the calculations were done by using the GAUSSIAN 98 program.[24]

III. RESULTS

A. Isomers responsible for the photoisomerization process: A ground states study

To determine which isomers are involved in the photoelectron spectroscopy experiment and hence interpret the photoisomerization process, it is necessary to check all possible candidate isomers. We have made an extensive exploration for the equilibrium geometries of the ground state for the neutral and anionic Al_3O_3 clusters and we find the conformations for these species are of rich diversity.[25] For the anions, 12 stable stationary points have been found. This indicates that the bonding in the species is rather flexible and potential energy surfaces are quite complex. The photoelectron spectroscopy experiments clearly show that small anion aluminum oxide isomers coexist. According to Boltzmann statistics, only the most energetically favorable structures are expected to be detached and are attributed to the observed spectra. Therefore, we focus on the three most stable structures of the $Al_3O_3^-$ species, as shown in Fig. 1. The geometrical and energetic information is listed in Tables I and II, respectively.

The three most stable isomers for $Al_3O_3^-$ are all of planar form with C_{2v} symmetry. The Book structure $^1A_1$ is the global minimum and the Kite structure lies higher in energy by 1.32 and 3.60 kcal/mol above using the B3LYP and MP2 methods, respectively. For the triplet Ring structure, we find that full optimization using both methods leads to the perfect D_{3h} symmetry being distorted into the C_{2v} symmetry. The Ring structure is 14.9 and 17.5 kcal/mol higher in energy

TABLE I. Geometries (angstrom, degree) of the three most stable isomers calculated at the B3LYP/6-31++G(p,d) level.

Method	Structure	State	R(1,6)	R(1,4)	R(2,4)	R(3,6)	θ(416)	θ(163)
MP2	Book	$^1A_1$	1.809	1.714	1.901	1.956	96.65	86.41
	Kite	$^1A_1$	1.747	1.738	1.892	1.706	87.48	97.62
	Ring	$^3B_2$	···	1.7661	1.7663	1.7657	57.77	62.26
B3LYP	Book	$^1A_1$	1.796	1.703	1.886	1.948	96.19	86.76
	Kite	$^1A_1$	1.738	1.723	1.877	1.699	87.98	97.09
	Ring	$^3B_2$	···	1.7541	1.7545	1.7538	57.21	63.08

than the Kite structure using B3LYP and MP2 methods respectively. We note that energy differences may be overestimated due to the different techniques used to describe these two states (i.e., the closed-shell restricted wave functions for singlet and open-shell unrestricted wave functions for the triplet state).

Electron affinities (EAs), defined as the difference in total energies between the neutral and the anion species, correspond to the position of the band in the photoelectron spectra associated with the given molecule. The difference between adiabatic EA and vertical EA correspond to the bandwidth.[26] Our EAs results as listed in Table II, show that B3LYP results are in better agreement with the experimental data than MP2 results. The latter method underestimates the EA values consistently. Our calculated EAs for the Book structure are in good agreement with the experimental data, suggesting that most energetically favorable Book structure is responsible for the strongest peak X in the photoelectron spectra. However, the Kite and the Ring structures provide very similar EA values. This means that the X' peak can be either attributed to the Kite structure or the Ring structure or both. So EA calculations alone cannot exclude the possibility of the existence of the Ring structure in the photoelectron spectroscopy experiment.

To resolve this dilemma, vibrational frequency analysis was performed, as it often serves as a direct tool for molecular recognition. IR absorption spectra and Raman scattering spectra are both common techniques for this purpose. The calculated frequencies with the symmetry group, the IR intensity, and Raman activity are complied in Table III. Experiment shows two active modes for the X band; one is centered at $\sim 610(60)$ cm^{-1}, and the other one is centered at $\sim 325(60)$ cm^{-1}. These two frequencies can be assigned to our calculated two modes at 575.5 cm^{-1} and 360.3 cm^{-1} for the Book structure since they have large IR intensity and Raman activity. Both of them have B_2 symmetry and vibrate on the molecular plane. This fact strengthens the evidence that the X band originals from the Book structure. So we conclude that the Book structure serves as the reactant for the photoisomerization process in photoelectron spectra. The other observed vibrational frequency for the X' band is centered at $\sim 720(60)$ cm^{-1}. There is no vibrational frequency in this region for the Kite structure. The most easily observed vibrational frequency for the Kite structure is either 1044 cm^{-1} (A_1) or 539 cm^{-1} (A_1). This mode can be attributed to the 761.7 cm^{-1} (A_1) or 762.1 cm^{-1} (B_2) of the triplet Ring structure, since both have very large Raman activity and large IR intensity. This agreement shows that the triplet Ring structure is involved in the photoelectron spectroscopy experiment and indicates that the inclusion of the Ring structure is necessary for understanding the photoelectron spectra change under hotter source conditions and stronger laser fluence.

Details of the electronic configuration are useful in the analysis of the electronic transition, and can help us to understand the photoisomerization process. MP2 and B3LYP methods give the same electronic configuration for each of the isomers. For the Book singlet state the configuration is $[\text{core}](2B_1)^2(1A_2)^2(6A_1)^2(5B_2)^2$; for the Kite singlet state the configuration is $[\text{core}](2B_1)^2(1A_2)^2(7A_1)^2(4B_2)^2$;

TABLE II. Calculated total energies, zero-point energies (ZPE), electron affinities,[a] and HOMO-LUMO gaps for the three most stable isomers of $Al_3O_3^-$.

Method	Structure (symmetry, state)	Total energy (a.u.)	ZPE (kcal/mol)	AEA (eV)	VEA (eV)	LUMO-HOMO (eV)
MP2	Book (C_{2v}, $^1A_1$)	−951.344 103	8.23	2.48	2.66	7.01
	Kite (C_{2v}, $^1A_1$)	−951.338 370	8.11	1.76	2.04	5.52
	Ring (C_{2v}, $^3B_2$)	−951.311 236	7.95	0.85	0.92	4.17
B3LYP	Book (C_{2v}, $^1A_1$)	−953.307 372	7.97	2.64	2.78	3.26
	Kite (C_{2v}, $^1A_1$)	−953.305 275	7.85	2.12	2.39	1.88
	Ring (C_{2v}, $^3B_2$)	−953.280 842	7.60	2.11	2.16	1.92

[a]Adiabatic electron affinity (AEA), is defined as the difference in total energy between the optimized neutral and optimized anion; vertical electron affinity (VEA) is the energy difference between optimized anion and neutral at optimized geometry of the anion (Ref. 26). The photoelectron spectroscopy experimental values for electron affinities: one is AEA=2.80(2) eV, VEA=2.96(2) eV, corresponding to the strongest bond and most stable structure, can be well assigned to the singlet Book isomer. Another one is: AEA=2.07(2) eV, VEA =2.25(2) eV, can be assigned either to the singlet Kite isomer or triplet Ring isomer.

TABLE III. Calculated vibrational frequencies (cm^{-1}) and infrared (IR) intensities (km/mol) and Raman scattering activities ($A^{4/amu}$) for the most stable anion Al_3O_3 isomers at the B3LYP/6-31++G(p,d) level. Entries in bold are referred to directly in the text.

	Symmetry	B1	A2	A1	B1	**B2**	A1	B2	A1	B2	A1	A1	B2
	Frequency	118.9	162.5	211.8	335.7	**360.3**	413.7	454.9	530.6	**575.5**	683.3	734.8	994.7
Book	IR Intensity	20.7	0	1.62	15.4	**100.4**	0.98	3.4	165.5	**302.3**	77.1	5.3	209.1
Structure													
$^1A_1$	Raman Activity	5.63	2.77	43.2	7.03	**29.1**	24.8	0.6	418.7	**162.3**	250.4	86.6	35.0
	Symmetry	B1	A2	A1	A1	B2	A1	A1	A1	B2	**A1**	**B2**	B2
	Frequency	114.5	116.4	198.3	198.4	200.2	390.4	540.0	604.2	605.2	**761.7**	**762.1**	822
Ring	IR Intensity	0	0	7	0.01	8.1	0	0.01	142.7	146.5	**18.2**	**19.8**	0
Structure													
$^3B_2$	Raman Activity	99.4	101.7	648.4	0.09	653.4	55.4	181.9	647.4	656.9	**2376**	**2339**	0.02
	Symmetry	B2	B1	B1	B2	A1	B1	B2	A1	A1	B2	A1	A1
	Frequency	57.5	69.4	162.9	229.6	320.8	338.8	483.3	539.4	587.4	818.8	840.7	1044
Kite	IR Intensity	0.6	4.9	5.4	5.3	2.4	32.1	71.3	72.7	102.3	118.7	7.3	827.8
Structure													
$^1A_1$	Raman Activity	2.6	9.0	13.5	14.5	54.7	17.8	3.9	1172	477.2	2.9	269.6	237.0

and for the Ring triplet state the configuration is $[\text{core}](2B_1)^2(1A_2)^2(6A_1)^2(4B_2)^2(7A_1)^1(5B_2)^1$, where the core electronic configuration is $(2B_1)^2(1A_2)^2(9A_1)^2(6B_2)^2$. The electronic configuration for the Ring structure is obtained by promoting one electron form the B_2 orbital of the Book structure into A_1 orbital accompanied with a spin flip. However, it is unlikely to change the electronic configuration of Book structure into that of the Kite structure due to large difference between them.

The electronic frontier orbitals are active during the photochemical reaction. To a first level of approximation, the excited state arises by promoting an electron from the highest occupied molecular orbital (HOMO) to the lowest unoccupied molecular orbital (LUMO). And the energy difference between the HOMO and LUMO roughly matches the first photon excitation energy.[2] Our calculated HOMO-LUMO energy gaps are listed in Table II. Again, B3LYP provides more reliable values than MP2 for the $Al_3O_3^-$ clusters compared with the experimental excitation energy. The LUMO-HOMO value (from B_2 to A_1) for the singlet Book structure, 3.29 eV, compares well with the experimental photon energy 355 nm (3.49 eV).

A particularly interesting feature here is that for the Ring structure, the triplet $^3B_2$ state is more stable than the singlet $^1A_1$ state by 2.62 eV and 2.83 eV using B3LYP and MP2, respectively. Note this is the only case of a stable triplet in all of the 12 isomers of the $Al_3O_3^-$ cluster. More interesting, both B3LYP and MP2 methods show that rerelaxation of the converged Ring structure on the singlet energy surface leads gradually into the Book structure and rerelaxation of the converged Book structure on the triplet energy surface leads gradually into the Ring structure. This important behavior can be more clearly demonstrated by mapping the local triplet and singlet potential energy surface along the distance of Al(1) and O(6) via partial relaxation employing the internal coordinates technique as shown in Fig. 2. For each structure point, only $R(1,6)$ is fixed, while all other geometric parameters are fully relaxed. It clearly shows that on the ground state, this system can be regarded as a bistable system; in the singlet ground state, the system exists as the Book structure, while in the triplet ground state, it changes into the Ring structure.

To understand this unique behavior, we performed natural population analysis to check the charge distribution and charge transfer during the process. Four states are studied: optimized singlet Book I, triplet Book II, optimized triplet Ring III and singlet Ring IV. II has the exactly same geometry as I but with different spin multiplicity. The same is true for III and IV. The natural electronic configuration and natural charge are compiled in Table IV, along with the Mulliken total atomic charge. Consistently we find the value of the natural population on Al is positive and on the O atom is negative. This not surprisingly shows that the charge is transferred from Al atoms to O atoms. While the values of natural population on O atoms remain nearly unchanged, the values on Al vary depending on the coordination and state. In I, the natural population value on Al(1) is much larger than the ones on Al(2) and Al(3). This is because the Al(1) atom is attached to three O atoms while Al(2) and Al(3) atom are both attached by two O atoms respectively. This difference is significantly decreased in II. The natural electron configurations show that in II, the number of the electrons in the $3s$ and $3p$ shell of Al(1) have increased while the number in $3s$ shell of Al(2) and Al(3) have decreased compared with I. Force analysis on the constrained structure II shows that there is strong repulsive force on Al(1) and O(6) along the $R(1,6)$, as well as a strong trend for O(4) and O(5) to move away from Al(1). These results agree with the Mulliken atomic charge analysis. Note that the Mulliken atomic charge on Al(1) in II is negative due to charge transfer from Al(2) and Al(3). We are not surprised at above result, i.e., that upon removal of the constraint the geometry may be driven into structure III, along with a decrease in energy. Similar analysis can be applied to the Ring structure III and IV. We find that the electronic charge distributes nearly evenly on the three Al atoms in III. This suggests that the added stability of the triplet III over the singlet IV is due to the resonance or delocalization of the electrons in the bonding network over the six atoms.[27]

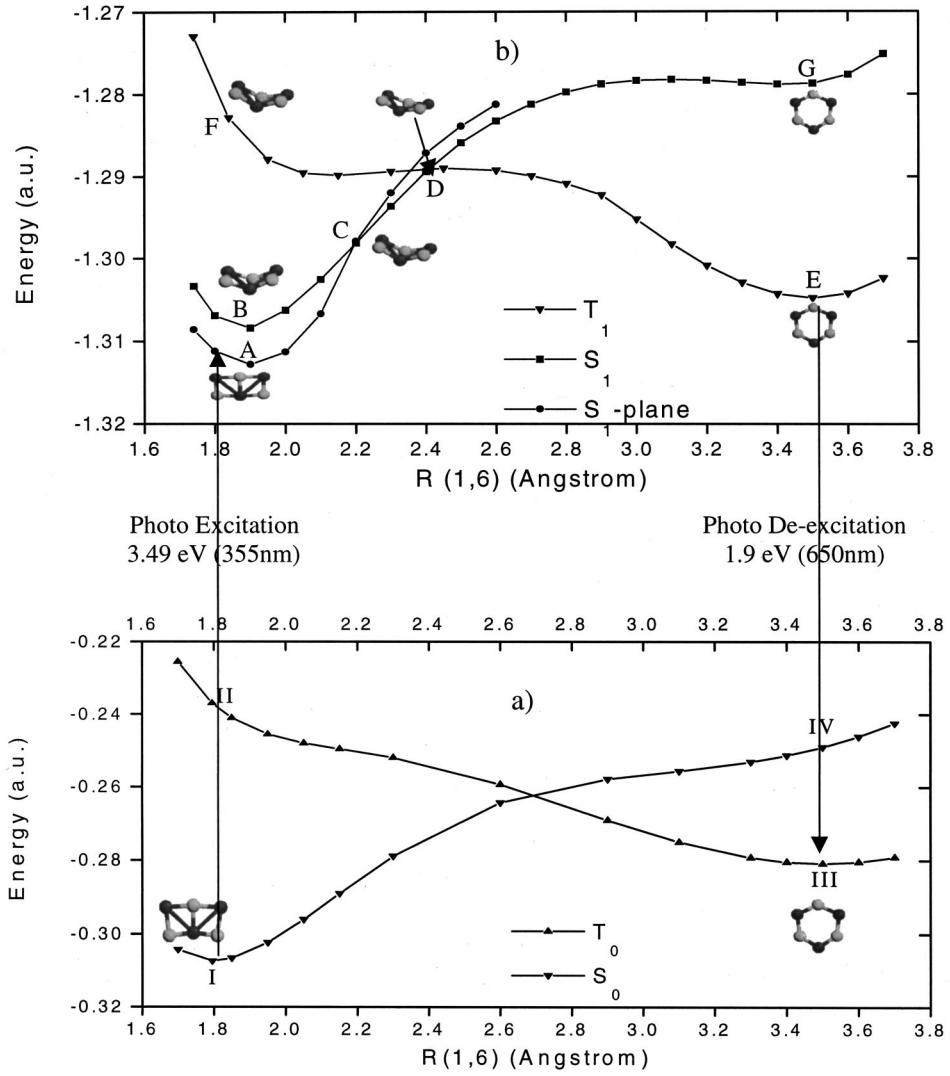

FIG. 2. Potential energy curves along $R(1,6)$ for (a) the electronic ground states and (b) the T_1/S_1 excited states. It demonstrates the photoisomerization from the Book structure to the Ring structure. Energies for ground states by B3LYP are relative to -953 a.u. and the energies for excited states by CI-singles are relative to -950 a.u. Vertical excitation and de-excitation energies are calculated by CASSCF.

From the above results, we see that the ground state calculations strongly suggest that the photoisomerization process observed in the photoelectron spectra experiment occurs between the singlet Book structure and the triplet Ring structure. Moreover, our ground state results indicate such a process may be reversible. However, before drawing such a conclusion, an excited state study must be performed since such photoinduced processes can only happen in the electronic excited states.

B. Photoisomerization mechanism in the $Al_3O_3^-$: An excited states study

While the ground states studies above provide insight into the reaction starting point, an excited state study is necessary for a description of the reaction process. Two excited state theoretical methods, CI-singles and CASSCF are employed here. From the ground state study, both the singlet and triplet excited states for the Book and Ring structure are believed to be involved in the photoisomerization process, hence we only consider the two low-lying excited states, S_1 and T_1. To understand the nature of the process, partial optimization was performed to describe the energy surface in the local region along the reaction pathway. The S_1 and T_1 electronic excited state geometries have been optimized at the 20-fixed $R(1,6)$ distances, corresponding to 20 steps of 0.1 Å from the Book to Ring structure. For each point, vibrational frequency analysis is used to guide the reoptimization if an imaginary frequency exists. We have obtained some nonplanar intermediate structures on these two excited energy surfaces. The importance of the utilization of the frequency analysis here is to expand the one-dimensional mapping into two-dimensional energy surface explorations. Due to the well known intrinsic convergence difficulties in the CASSCF method, this formidable mapping task was achieved by the computationally less-expensive CI-singles method. However, for the most important structures and the vertical excitation energy, more accurate CASSCF calculations were performed. The calculated PES mapping for the singlet and triplet ground states and the low-lying excited states is illustrated in Fig. 2. The optimized geometric data for the key structures are given in Table V. For the Book structure, CASSCF gives a very similar ground state geometry as those from B3LYP and MP2 and similar S_1 geometry as that from CI-singles. However, for the Ring structure, a large discrepancy exists between the two methods.

Similar to the ground state potential energy surface, the

TABLE IV. Natural population and natural electron configurations of the relative $Al_3O_3^-$ isomers at the B3LYP/6-31++G(p,d) level.

	Atom	Natural electron configuration	Natural population	Total atomic charge
Book-I	Al(1)	[core] $3s^{0.38}\ 3p^{0.20}\ 3d^{0.03}\ 4p^{0.17}\ 5p^{0.22}$	2.011	0.054
singlet	Al (2,3)	[core] $3s^{1.74}\ 3p^{0.49}\ 4s^{0.01}\ 3d^{0.01}$	0.751	−0.046
$^1A_1$	O(4,5)	[core] $2s^{1.87}\ 2p^{5.58}\ 3d^{0.01}$	−1.476	−0.375
	O(6)	[core] $2s^{1.87}\ 2p^{5.67}\ 3d^{0.01}$	−1.559	−0.213
Book-II	Al(1)	[core] $3s^{0.85}\ 3p^{0.59}\ 4s^{0.05}\ 3d^{0.03}\ 4p^{0.01}$	1.469	−0.215
triplet	Al (2,3)	[core] $3s^{1.33}\ 3p^{0.60}\ 3d^{0.01}\ 4p^{0.02}$	1.031	0.014
$^3B_2$	O(4,5)	[core] $2s^{1.88}\ 2p^{5.57}\ 3s^{0.02}\ 3p^{0.01}\ 3d^{0.01}$	−1.490	−0.28
	O(6)	[core] $2s^{1.87}\ 2p^{5.67}\ 3p^{0.01}$	−1.552	−0.252
Ring-III	Al(1)	[core] $3s^{1.15}\ 3p^{0.60}\ 4s^{0.01}\ 3d^{0.02}\ 4p^{0.01}$	1.214	−0.0424
$^3B_2$	Al (2,3)	[core] $3s^{1.15}\ 3p^{0.60}\ 4s^{0.01}\ 3d^{0.02}\ 4p^{0.01}$	1.211	−0.0437
	O(4,5)	[core] $2s^{1.87}\ 2p^{5.66}\ 3p^{0.01}\ 3d^{0.01}$	−1.545	−0.290
	O(6)	[core] $2s^{1.87}\ 2p^{5.66}\ 3p^{0.01}\ 3d^{0.01}$	−1.546	−0.289
Ring-IV	Al(1)	[core] $3s^{1.12}\ 3p^{0.41}\ 4s^{0.01}\ 3d^{0.02}\ 4p^{0.13}$	1.309	0.125
$^1A_1$	Al (2,3)	[core] $3s^{1.15}\ 3p^{0.65}\ 4s^{0.02}\ 3d^{0.02}\ 4p^{0.01}$	1.156	−0.148
	O(4,5)	[core] $2s^{1.88}\ 2p^{5.64}\ 3p^{0.01}\ 3d^{0.01}$	−1.532	−0.275
	O(6)	[core] $2s^{1.86}\ 2p^{5.69}\ 3d^{0.01}$	−1.558	−0.278
Kite	Al(1)	[core] $3s^{0.36}\ 3p^{0.18}\ 3d^{0.03}\ 4p^{0.17}\ 59^{0.19}$	2.072	−0.25
singlet	Al(2)	[core] $3s^{1.71}\ 3p^{0.47}\ 4s^{0.02}\ 3d^{0.01}\ 4p^{0.09}$	0.695	0.13
$^1A_1$	Al(3)	[core] $3s^{1.82}\ 3p^{0.36}\ 4s^{0.01}\ 3d^{0.01}$	0.80	−0.0058
	O(4,5)	[core] $2s^{1.88}\ 2p^{5.59}\ 3p^{0.01}\ 3d^{0.01}$	−1.488	−0.412
	O(6)	[core] $2s^{1.86}\ 2p^{5.72}$	−1.591	−0.05

S_1 surface has a valley that accommodates the singlet Book structure while the T_1 surface has a valley that accommodates the triplet Ring structure. Both the S_1 and T_1 curves change monotonically along the reaction pathway. In fact, full relaxation starting from the Book structure on T_1 surface leads to the Ring structure and full relaxation from Ring structure (with little initial distortion) on S_1 surface leads to the Book structure.

On the S_1 surface, in the vicinity of $R(1,6)=1.9$ Å, CI-singles shows the planar structure A has one imaginary frequency, and reoptimization lead to a bent structure B. However, B structure lies higher in energy by 0.14 eV over the A structure by CI-singles. Moreover, CASSCF vibrational frequency shows that A is a true minimum on the S_1 surface. The A structure is very similar to the I structure. According to the Franck–Condon principle, the nuclei remain essentially frozen at the equilibrium configuration of the ground state molecule during the transition. Thus we conclude that upon absorption of a photon, the ground state I will be promoted to the region near the A point (the so-called Franck–Condon region) rather than the B point. Our CASSCF calculated vertical excitation energy from S_0 to S_1 is 3.62 eV. This value is in good agreement with the photoelectron photon energy (355 nm, 3.49 eV), it is also roughly in line with the HOMO-LUMO energy gap for the ground state of the Book structure.

Near the C point with $R(1,6)=2.2$ Å, the bent structure is found to be energetically more favorable. So at this region, the planar reactant changes into nonplanar form accompanied by a state change from $^1A_1$ to $^1A'$. A nonplanar conical intersection of S_1/T_1 was found in the vicinity with $R(1,6)=2.4$ Å. This conical intersection occurs at a geometry

TABLE V. Geometries (angstrom, degree) of relative isomers by different approaches employing the 6-31++G(p,d) basis set.

Isomer (state)	Method	$R(1,6)$	$R(1,4)$	$R(3,6)$	$\theta(416)$	$\theta(163)$	$D(5162)$[a]
I ($^1A_1$)	B3LYP	1.796	1.703	1.948	96.19	86.76	180
	CAS	1.767	1.677	1.926	95.91	87.45	180
A ($^1A_1$)	CIS	1.90	1.739	1.819	87.20	89.33	180
	CAS	1.883	1.728	1.808	86.43	90.36	180
B ($^1A'$)	CIS	1.90	1.729	1.828	88.01	87.10	133.23
C ($^1A'$)	CIS	2.20	1.702	1.794	82.99	82.82	141.80
D ($^1A'$)	CIS	2.41	1.687	1.773	79.01	80.01	148.79
E ($^3B_2$)	CIS	3.50	1.687	1.754	58.34	62.07	180
	CAS	3.731	1.892	1.732	51.34	67.67	180
III ($^3B_2$)	CAS	3.742	1.922	1.725	47.89	80.33	180
	B3LYP	3.496	1.7541	1.7538	57.21	63.08	180
F ($^3A''$)	CIS	1.84	1.776	1.823	86.87	89.31	135.62
G ($^1A_1$)	CIS	3.3	1.673	1.749	61.92	65.92	180

[a]Dihedral angles, 180° means planar form.

which is characterized with $R(1,4)=1.69$ Å, $R(3,6)=1.77$ Å and, $D(4163)=149°$. This point is important to the photoinduced process because it serves as a bottleneck controlling the reaction direction. At this point, the two electronic states share same energy and very similar geometries. This twisted conical intersection point serves as a *funnel* geometry for spin inversion, and it is believed that such geometry is responsible for an efficient S_1/T_1 transition.[10] Around this turning point, the reactant will migrate from the S_1 ($^1A'$ state) surface to the T_1 surface ($^3A''$ state). This intersystem crossing is a nonradiative process. The CI-singles calculated energy barrier height from A to D is about 0.6 eV. This barrier separates intermediate A on the excited state S_1 from the S_1/T_1 conical intersection point D. This energy barrier can be overcome by thermal energy in the cluster. This value may be not quantitatively accurate, unfortunately, as we failed to refine this value due to difficulties characterizing the D point at the CASSCF level. The T_1 state surface is quite flat in the region with $R(1,6)$ varying from 2.2 to 2.6 Å and the cluster is very flexible. After passing the turning point D, the dihedral angle continues to become larger, and at about $R(1,6)=2.7$ Å, the bent structure changes back into the planar structure accompanied by the electronic state changing from $^3A''$ into $^3B_2$ simultaneously. On the T_1 surface, no barrier is found, so the reactant can readily reach the minimum Ring intermediate E point with $R(1,6)=3.52$ Å. The E point is on the first triplet excited state for the Ring structure and has a very similar geometry compared to III. This state is energetically unstable with respect to the ground state. It has a strong tendency to undergo a radiative transition to the ground state. Such emission is referred to as fluorescence. Since there is no change of spin multiplicity, the transition is spin-allowed. This deexcitation process is an internal conversion (IC) and is strongly allowed and occurs on relatively short timescales with a high efficiency. Our CASSCF calculated vertical excitation energy from III to T_1 is 1.92 eV, again, it is roughly in line with the HOMO-LUMO energy gap for the ground state triplet Ring structure (1.9 eV). Therefore the radiated phonon frequency is predicted at about 645 nm. This important feature is expected to be confirmed by further experiment.

Based on the above model, one can readily understand the fact that such a photoinduced process will be significantly enhanced under hot source conditions in the photoelectron spectra experiment. First, a higher temperature will increase the population of the energetically unfavourable species. In the present case, it will increase the concentration of the reactant triplet Ring isomer. Furthermore, a hot condition will increase the amount of thermal energy in the cluster available to overcome the energy barrier. Also, a stronger laser beam will intensify this process because it will increase the possibility of this photoinduced process.

So far, based on our results, we can understand the photoisomerization observed in experiment. A particularly interesting question concerns the possibility of the reversibility of this photochemical reaction. Based on our study of the ground state and excited state PES, we see the reverse isomerization is possible and can be described as follows: Upon absorption a photon with wavelength at 645 nm, the ground triplet Ring III will be levered to the side of the E point on the T_1 surface. After overcoming an energy barrier of 0.42 eV (at CI-singles level), it will reach the nonplanar conical intersection D point and cross into the singlet S_1 surface. From there it can readily reach the minimum A point. This electronic excited state will release the extra energy by emitting a photon at about 350 nm and terminate at the ground state I.

IV. DISCUSSION

The photoexcitation dramatically changes the electron distribution and the excited state has very different properties compared to the ground state. In fact, in our exploration of all the possible stationary points, no nonplanar structure was found in the electronic ground state. Reoptimization of the nonplanar form found in the excited state all lead to the planar structures predicted by B3LYP.

Although B3LYP and MP2 provide very similar optimized structures and the same electronic configurations for the species studied here, our ground state calculations reveal that the B3LYP-DFT method offers a better description for the small aluminum oxide species by comparison with experiment. It is perhaps not surprising that B3LYP predicts reasonable values for properties obtained from electronic ground states (ZPE, AEA, and VEA) as the functional is semiempirical in nature with 3 adjustable parameters chosen to reproduce electronic ground state properties of a wide range of simple molecular structures.[28] As found previously, the DFT approach is quite robust against spin contamination of the wave function when dealing with systems of different spin multiplicity.[29] Furthermore, as already mentioned, Table II also shows the LUMO-HOMO gaps predicted with B3LYP to be much closer to experimental excitation energies compared to MP2. The MP2 LUMO-HOMO gaps are very close to the HF values (6.95, 5.43, and 5.10 eV for the Book, Kite, and Ring structures, respectively) that consistently overestimate the electron excitation energies. The B3LYP functional consists of a mixture of the exact exchange functional and a GGA functional, the former overestimates single electron excitation energies while the latter is known to underestimate them. It is then perhaps not surprising that a mixture of the two produces LUMO-HOMO gaps in reasonable agreement with experimentally observed excitation energies. From our present study, it seems that B3LYP takes into account most of the important dynamical and nondynamical correlation effects. Another advantage of the B3LYP method is that it reduces the computational time and memory requirements.

The CI-singles method is a first-level method for modeling excited states and is regarded as zeroth-order treatment for the excited states. The CI-singles method uses SCF-HF orbitals for the excited state while CASSCF calculation uses optimized orbitals (the active space) appropriate for the excited state. Thus CASSCF provides better description for the electronic excited state. Although CI-singles is regarded as quite crude, it is qualitatively correct here and it yields much insight into the photoisomerization process in the $Al_3O_3^-$ cluster system. We also note that the newly proposed *improved virtual orbital-complete active space configuration*

interaction method (IVO-CASCI) (Ref. 30) could be an ideal approach to improve quantitatively the excited state study here.

Interestingly, our study suggests that one can regard the Book structure and Ring structure as a unique system whose structure is strongly dependent on its spin multiplicity. Such a system, in both the ground state and excited states (S_1 and T_1), can only exist as the Book structure in a singlet state, and as the Ring structures in a triplet state. A most interesting feature of this system is that these two conformations, in principle, can be exchanged upon absorption or emitting radiation. This novel property may inspire applications by utilizing alternation of the chemical structure in terms of photoswitching and photon-mode high-density information storage devices.[5]

Structurally, the most prominent difference between the Book Structure and the Ring structure lies at the bond length $R(1,6)$. The isomerization can be regarded as a process by first stretching then breaking of Al(1)–O(6) bonds. This is another example where bond cleavage happens upon irradiation.

V. CONCLUSION

We have presented a quantitative picture for understanding the photoisomerization process in $Al_3O_3^-$ clusters by means of quantum chemistry calculations. Possible intersystem crossing pathways have been outlined by geometry optimization on the relevant potential energy surfaces. Combining the results for both ground states and low-lying excited states, we summarize our main results as follows:

(1) The photoinduced process occurs between the singlet Book structure (C_{2v},$^1A_1$) and the triplet Ring structure (C_{2v},$^3B_2$). Another energetically favorite Kite isomer (C_{2v},$^1A_1$) may coexist in the photoelectron spectroscopy experiment, but it is not involved in this photoinduced reaction. Our electron affinity values, the vibrational frequency analysis, and electronic structure results support this conclusion.

(2) We have mapped in detail the local ground state and triplet state potential energy surfaces along the bonding length $R(1,6)$, spanning from 1.8 Å to 3.6 Å by utilizing the partial relaxation technique. A nonplanar conical intersection between S_1 and T_1 occurs with $R(1,6)$ at about 2.4 Å. This point controls the reactant transfer from the S_1 surface to T_1 surface. The calculated vertical excitation energy is 3.62 eV at CASSCF level, in good agreement with the experimental value (3.49 eV) and roughly in accordance with the HOMO-LUMO energy gap of the singlet Book structure (3.29 eV).

(3) Beyond the experimental results, we predict, in principle, this photoisomerization process is reversible. Upon absorption a phonon of 1.92 eV energy, the triplet Ring structure is expected to change back into the singlet Book structure.

(4) The singlet Book structure and the triplet Ring structure can be regarded as a unique bistable system. Such system has the very interesting property that in both the ground state and excited states (S_1 and T_1), such system can only exist as the Book conformation on singlet state energy surfaces, and as the Ring conformation on triplet state energy surfaces.

ACKNOWLEDGMENTS

X.Y.C. gratefully acknowledges the financial support of ORS scheme. All calculations were performed at the University of Salford using the High Performance Computing facilities supported by HEFCE (U.K.) and IBM Ltd.

[1] J. A. Barltrop and J. D. Coyle, *Excited States in Organic Chemistry* (Wiley, New York, 1975).
[2] A. Gilbert and J. Baggott, *Essentials of Molecular Photochemistry* (Blackwell Scientific, Oxford, 1991).
[3] V. Molina, M. Merchan, B. O. Roos, and P. Malmqvist, Phys. Chem. Chem. Phys. **2**, 2211 (2000).
[4] M. Woeller, S. Grimme, S. D. Peyerimhoff, D. Danovich, M. Filatov, and S. Shaik, J. Phys. Chem. A **104**, 5366 (2000).
[5] J. K. Agyin, L. D. Timberlake, and H. Morrison, J. Am. Chem. Soc. **119**, 7945 (1997); M. Kurihara, T. Matsuda, A. Hirooka, T. Yutaka, and H. Nishihara, *ibid.* **122**, 12373 (2000), and references therein.
[6] Z. F. Liu, K. Hashimoto, and A. Hujishima, Nature (London) **347**, 658 (1990); T. Ikeda and O. Tsutsumi, Science **268**, 1873 (1995); F. Kulzer, S. Kummer, R. Matzke, C. Brauchle, and T. Basche, Nature (London) **387**, 688 (1997).
[7] M. J. Bearpark, M. Olivucci, S. Wilsey, F. Bernard, and M. A. Robb, J. Am. Chem. Soc. **117**, 6944 (1995).
[8] W. Fuss, S. Lochbrunner, M. Muller, T. Schikarski, W. E. Schmid, and S. A. Trushin, Chem. Phys. **232**, 161 (1998).
[9] P. Weber, J. R. Reimers, J. Phys. Chem. A **103**, 9830 (1999).
[10] F. Bernardi, M. Olivucci, and M. A. Robb, Chem. Soc. Rev. **25**, 321 (1996).
[11] M. Klessinger, Angew. Chem. Int. Ed. Engl. **34**, 549 (1995).
[12] P. Chaquin, M. E. Alikhani, M. Bahou, L. S. Mazzuoli, and A. Schriver, J. Phys. Chem. A **102**, 8222 (1998).
[13] J. Manz, K. Sundermann, and R. de. Vivie-Riedle, Chem. Phys. Lett. **290**, 415 (1998).
[14] M. Hartmann, J. Pitter, and V. B. Koutecky, J. Chem. Phys. **114**, 2123 (2001).
[15] V. B. Koutecky, M. Hartmann, J. Pitter, and H. D. Van, Int. J. Quantum Chem. **84**, 714 (2001).
[16] H. Wu, X. Li, X. B. Wang, C. F. Ding, and L. S. Wang, J. Chem. Phys. **109**, 449 (1998).
[17] T. K. Ghanty and E. R. Davidson, J. Phys. Chem. A **103**, 8985 (1999).
[18] A. V. Nemukhin and F. Weinhold, J. Chem. Phys. **97**, 3420 (1992).
[19] C. Møller and M. S. Plesset, Phys. Rev. **46**, 618 (1934).
[20] A. D. Becke, Phys. Rev. A **38**, 3098 (1988).
[21] C. Lee, W. Yang, and R. G. Parr, Phys. Rev. B **37**, 785 (1988).
[22] J. B. Foresman, M. Head-Gordon, J. A. Pople, and M. J. Frisch, J. Phys. Chem. **96**, 135 (1992).
[23] P. E. Seigbahn, A. Heiberg, B. O. Roos, and B. Levy, Phys. Scr. **21**, 323 (1980); B. O. Roos, P. R. Taylor, and P. E. Seigbahn, Chem. Phys. **48**, 157 (1980); N. Yamamoto, T. Vreven, M. A. Robb, M. J. Frisch, and H. B. Schlegel, Chem. Phys. Lett. **250**, 373 (1996).
[24] M. J. Frisch, G. W. Trucks, H. B. Schlegel *et al.*, GAUSSIAN 98 Gaussian, Inc., Pittsburgh, PA, 1998.
[25] X. Y. Cui, and I. Morrison (unpublished).
[26] L. S. Wang, J. B. Nicholas, M. Dupuis, H. Wu, and S. D. Colson, Phys. Rev. Lett. **78**, 4450 (1997).
[27] R. L. Dekock and H. B. Gray, *Chemical Structure and Bonding* (University Science, New York, 1989).
[28] A. D. Becke, J. Chem. Phys. **107**, 8554 (1997), and references therein.
[29] S. Grimme, M. Woeller, S. D. Peyerimhoff, D. Dannovich, and S. Shaik, Chem. Phys. Lett. **287**, 601 (1998).
[30] D. M. Potts, C. M. Taylor, R. K. Chaudhuri, and K. F. Freed, J. Chem. Phys. **114**, 2592 (2001).